frontiers in Materials

ORIGINAL RESEARCH
published: 09 November 2020
doi: 10.3389/fmats.2020.574924

Effect of Bamboo Flour on Flame Retardancy and Smoke Suppression of Polypropylene/Ammonium Polyphosphate Composites

Yide Liu[1], Hongzhou Li[1], Qinghua Chen[1,2]*, Fubin Luo[1] and Changlin Cao[1]*

[1]College of Environmental Science and Engineering, Fujian Normal University, Fuzhou, China, [2]Fujian Polytechnic Normal University, Fuqing, China

In this paper, the flame-retardant Polypropylene (PP) composites were prepared by melt blending. Ammonium Polyphosphate (APP) and bamboo flour (BF) were selected as flame retardant and smoke suppressant of the composite material. Among them, BF as a synergist can effectively improve the flame retardancy and smoke suppression effect of PP/APP composites. The effects of BF on the mechanical properties, crystallization behavior, thermal degradation, flame retardancy, and especially the smoke suppression effect of PP/APP composite materials were studied. thermogravimetric analysis, limiting oxygen index, cone calorimetry, scanning electron microscopy and other characterization methods were used to study the thermal stability, flame retardancy and combustion characteristics of the composites and the microscopic morphology of carbon residue. Experimental results showed that when the total addition amount of APP/BF (2:1) in PP55/APP30/BF15 composite is 45%, the residual carbon had more specific surface area and micro-pores, which causes the composite to have the best smoke suppression effect. The PHRR of the PP55/APP30/BF15 composite was reduced to 308.2 kW/m^2 and the amount of carbon residue was 25%. The continuous carbon layer, formed during combustion can effectively protect the matrix material and prevent the transfer of heat.

Keywords: polypropylene, ammonium polyphosphate, bamboo flour, smoke suppression, flame retardancy

OPEN ACCESS

Edited by:
Bin Yu,
University of Southern Queensland, Australia

Reviewed by:
Jun Sun,
Beijing University of Chemical Technology, China
Wei Yang,
Hefei University, China
Gang Tang,
Anhui University of Technology, China

****Correspondence:***
Hongzhou Li
lihongzhou@fjnu.edu.cn,
Qinghua Chen
cqhuar@fjnu.edu.cn

Specialty section:
This article was submitted to Polymeric and Composite Materials, a section of the journal Frontiers in Materials

Received: *22 June 2020*
Accepted: *18 August 2020*
Published: *09 November 2020*

Citation:
Liu Y, Li H, Chen Q, Luo F and Cao C (2020) Effect of Bamboo Flour on Flame Retardancy and Smoke Suppression of Polypropylene/Ammonium Polyphosphate Composites. Front. Mater. 7:574924. doi: 10.3389/fmats.2020.574924

INTRODUCTION

Polypropylene (PP) is a thermoplastic polymer with excellent comprehensive properties, and it is now widely used in construction, packaging, transportation and furniture (Kumar et al., 2017). Due to the poor heat resistance and the poor flame retardancy of PP, its application is limited to a relatively low temperature (Abu Bakar et al., 2010; Xu et al., 2019). At present, halogen-free flame-retardant technology is a research focus in the field of flame retardancy for environmental and health consideration. In this field, many scholars are focusing on 2D flame retardant materials, such as transition metal compounds because they have excellent catalytic oxidation properties (Kong et al., 2019; Shi et al., 2019; Yu et al., 2020), but the preparation of such flame retardants is usually more complicated and the actual cost of application is higher. In addition, phosphorus-containing flame retardants are often used for flame retardant treatment of polymer because they are rich in phosphorus elements, such as melamine pyrophosphate, aluminum diethylphosphinate, etc.

(Tang et al., 2020b; Tang et al., 2020c). This type of flame retardant usually needs to be compounded with carbon sources such as expanded graphite (Tang et al., 2020a). Most of them are additive-type flame retardants, which require a large amount of addition. Therefore, it will increase the cost of flame-retardant treatment. In summary, the development of low-cost environmentally friendly additive-type flame retardants will be of great significance to actual production.

Phosphorus-based intumescent systems have a wide application range and high flame-retardant efficiency, so they are suitable for polymers flame retardant (Yang et al., 2011; Wang et al., 2012). Ammonium polyphosphate (APP) is a typical representative of halogen-free flame retardants, which has the advantages of high efficiency and is environmentally friendly. In addition, the production process of APP is simple, and it is widely used in the market. Therefore, APP as an intumescent flame retardant is widely used in polymer materials (Zhou et al., 2011; Zhao et al., 2018; Dong et al., 2020; Wu et al., 2020a; Wu et al., 2020b; Xu et al., 2020). When APP is pyrolyzed, it will promote the dehydration of the matrix and be decomposed by heat to form carbides and phosphoric acid, and then cover the surface of the matrix with a carbon layer. At the same time, APP is decomposed by heat to generate NH3 and H2O, which can dilute the concentration of flammable gas in the air, thereby taking effect as a flame retardant (Wang et al., 2020). The addition of APP into the PP matrix can improve the flame retardancy of PP, nevertheless the smoke suppression performance of this composite material is poor. We found that when bamboo flour (BF) and APP were added in PP with a certain proportion, the smoke suppression effect of PP is improved.

Bamboo has a short growth cycle and wide range of planting. Therefore, bamboo resources are abundant. As a biomass material, BF has the advantages of good thermal stability, low cost and degradability (Nie et al., 2013). Because BF has so many advantages, its application is increasingly extensive (Lee et al., 2009; Chattopadhyay et al., 2011; Li et al., 2019; Fang et al., 2020). However, the effect of flame retardancy via adding BF and APP into PP and studying of its smoke suppression performance has rarely been reported.

In this study, BF and APP were used as a compound flame retardant for PP flame retardant modification, and an environmentally friendly PP composite with flame retardancy was prepared by a blending process. Flame retardancy and smoke suppression tests were carried out on the prepared PP composites by the limiting oxygen index (LOI), the vertical burning method (UL-94), and the cone calorimeter test, and the thermal stability of materials by thermogravimetric analysis (TGA). Then, the scanning electron microscopy (SEM) was used to analyze the morphology of the samples after the cone test.

EXPERIMENT

Materials

Polypropylene (PP, PPR-4220, random copolymer, MFI: 0.4 g/10 min) was supplied by China Petrochemical, Co., Ltd. (China). Ammonium polyphosphate (APP, Degree of polymerization ≥1,000) was bought from Shandong Taixing New Material, Co., Ltd. (China). BF was bought from Quanzhou Baixin Biotechnology, Co., Ltd. (China), and the particle size of BF is about 60 μm.

The Preparation of Samples

PP, APP and BF were dried in a blast drying oven (DHG-9070A) at 80°C for 12 h before the experiment. First, APP and BF were added in a small high-speed mixer (FW177) at a fixed speed of 500 rpm and were mixed for 10 min to obtain a compound flame retardant. Second, the samples were prepared by mixing the compound flame retardant with PP in a two-roll mill (ZG-200) at 190°C for 15 min, with a roller speed of 30 rpm. The components of samples are shown in **Table 1**. Third, the right amount of material was weighed and put in a flat vulcanizing machine (ZG-80T), removing the samples after being pressed for 15 min under 10 MPa pressure. Finally, the samples were dried at room temperature for 24 h, and various test splines were cut through a universal sample preparation machine (WZY-240).

Mechanical Properties Test

The tensile strength test and flexural strength test were performed on a CMT-4104 universal mechanical testing machine (produced by Shenzhen Xinsansi Material Testing, Co., Ltd), where the tensile speed is set as 50 mm/min, and the bending speed is 2 mm/min. The simple supported beam impact test was performed on a ZBC500 testing machine (produced by Shenzhen Xinsansi Material Testing, Co., Ltd.).

Cross-Section Topography

The samples were brittle after being frozen in liquid nitrogen and a part of the complete section of the samples was cut out. Then, the sections were subjected to gold spraying treatment and the cross-section morphology was observed at 5 kV by a Regulus 8100 cold field emission scanning electron microscope (produced by Japan Hitachi Company).

DSC Test

The Q20 differential scanning calorimeter (TA Instruments) was used to study the melting and crystallization behavior of the samples. Approximately 7 mg of the sample was weighed and placed in an alumina crucible. First, the samples were heated from 30 to 200°C at a rate of 10°C/min and equilibrated for 5 min to eliminate thermal history under nitrogen atmosphere protection. Then, the temperature was reduced to 30°C at a rate of 10°C/min and equilibrated for 5 min. Finally, the samples were heated to 200°C at a rate of 10°C/min and the DSC curve was recorded.

Flame Retardancy Test

The LOI was measured by a HC-2C oxygen index meter (Nanjing Shangyuan Analysis Instrument Company, China). The LOI test was performed according to the ASTM D2863-77. The LOI refers to the volume fraction concentration of oxygen just supporting combustion in the oxygen and nitrogen mixed gas. The specimen dimensions were 125 mm × 6.5 mm × 3.2 mm and five samples for each group were tested.

TABLE 1 | The components of samples.

Samples	PP	PP70/APP30	PP70/BF30	PP65/APP30/BF5	PP60/APP30/BF10	PP55/APP30/BF15
PP/%	100	70	70	65	60	55
BF/%	0	0	30	5	10	15
APP/%	0	30	0	30	30	30

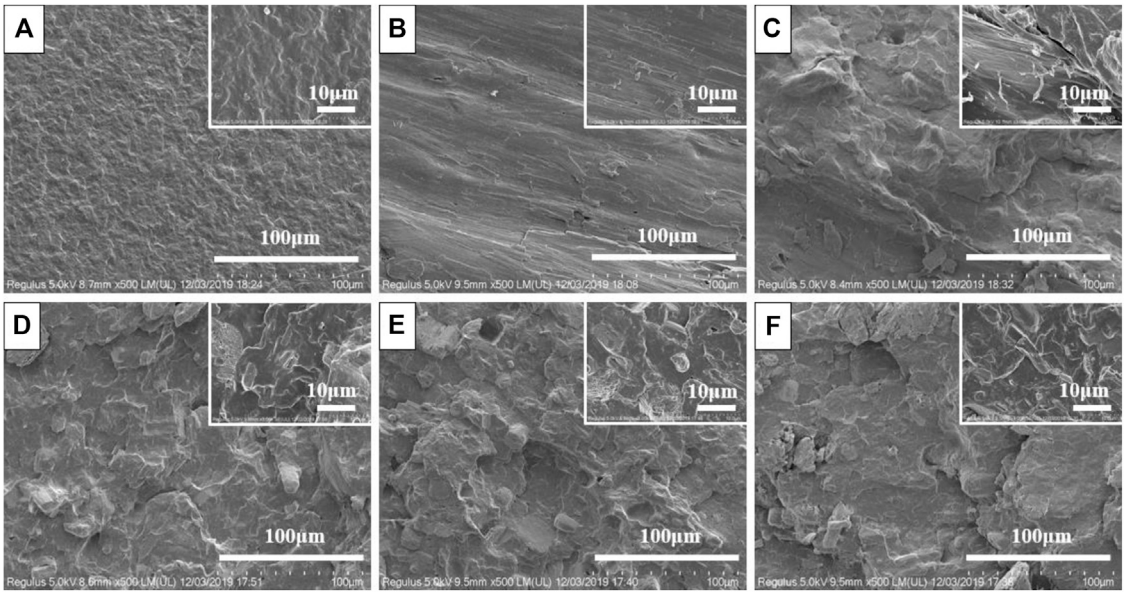

FIGURE 1 | SEM micrographs of PP and composites. (**(A)** PP; **(B)** PP70/APP30; **(C)** PP70/BF30; **(D)** PP65/APP30/BF5; **(E)** PP60/APP30/BF10; **(F)** PP55/APP30/BF15).

The UL-94 vertical burning test was performed on a CZF-4 vertical burning tester (Nanjing Shangyuan Analysis Instrument Company, China), according to ASTM D635-77. The specimen dimensions used for the test were 125 mm × 13 mm × 3.2 mm.

Thermal Stability Test

The TGA was carried out using a SDT Q600 (TA Instruments) thermo-analyzer instrument at a linear heating rate of 10°C/min under a nitrogen atmosphere, and the test temperature ranged from 30 to 700°C. Samples with a mass of about 5–10 mg were weighed in a clean alumina crucible.

Cone Calorimeter Test

The cone calorimeter test is a method that can effectively reflect the fire level. The materials were tested for burning performance using a cone calorimeter (FTT classic, United Kingdom), and the specimen dimensions were 100 mm × 100 mm × 4 mm. The test was carried out under the ISO 5660-1 standard with a heat flow of 35 kW/m^2.

Scanning Electron Microscopy Analysis

The microscopic morphology of the char residues after the cone test was examined by a Regulus 8100 cold field emission scanning electron microscope (produced by Japan Hitachi Company).

RESULTS AND DISCUSSION

Section Characterization

In order to analyze and study the dispersion of flame retardants in PP, the splines were brittlely broken under the condition of liquid nitrogen, and the cross-sectional morphology of the samples was analyzed by SEM. **Figure 1** is the SEM images of the samples at different magnifications. As can be seen from **Figure 1A**, the section of pure PP is relatively flat, with a lamellar structure, and behaves as a typical ductile fracture. After joining APP, the sectional view is shown in **Figure 1B**. The cross section is smooth and tidy, showing a uniform shape which is a typical brittle fracture. As can be seen from **Figure 1C**, fibrous BF is evenly wrapped by PP and disperses well. Comparing **D, E, F** in **Figure 1**, it can be seen that the interface becomes rough and fuzzy when APP and BF were mixed, and some flours were pulled out. This is due to the agglomeration of APP and BF, which reduces the compatibility with the matrix. At the same time, larger roughness caused a larger gap between the flame retardant and the matrix PP. If an external force was applied, these gaps will form stress concentrations.

Mechanical Properties

The tensile strength, flexural strength and impact strength of the samples are shown in **Figure 2-4**, respectively. It can be seen from

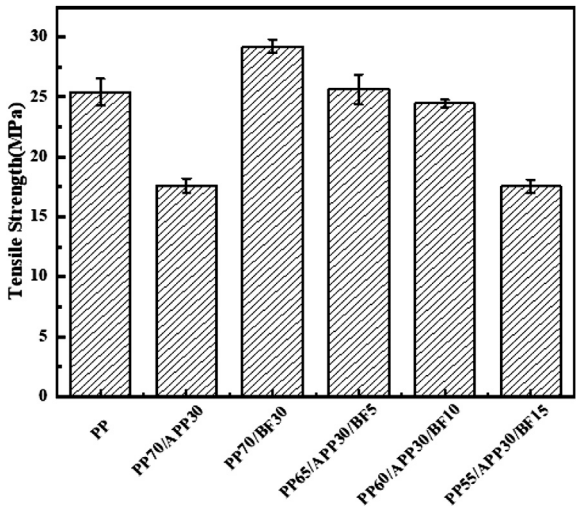

FIGURE 2 | Tensile strength of PP and composites.

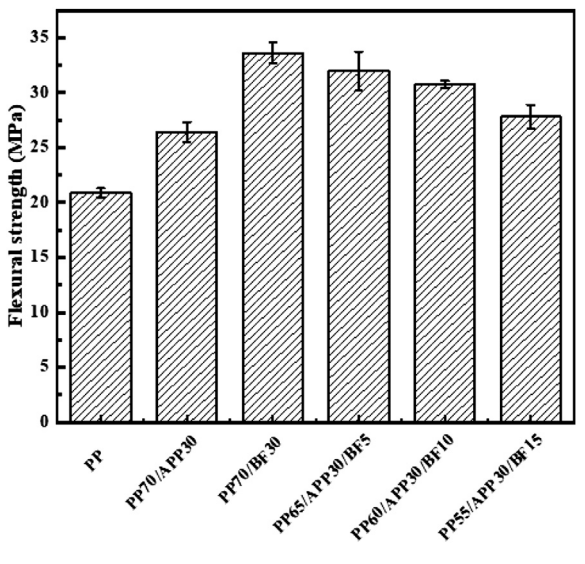

FIGURE 3 | Flexural strength of PP and composites.

Figure 2 that the tensile strength of PP was 25.4 MPa. After adding APP, the tensile strength decreased sharply due to APP agglomeration. When 30% BF was added, the tensile strength of the PP70/BF30 sample reached 29.3 MPa, which might be ascribed to BF having a good strengthening effect. Among the PP65/APP30/BF5, PP60/APP30/BF10, and PP55/APP30/BF15 samples, the mechanical properties of the three samples were decreased when the compound flame retardants were added. This is due to the poor compatibility between flame retardants and the matrix. However, the addition of BF could properly enhance the flexural strength of PP/APP composites, as seen from the result of samples PP65/APP30/BF5, PP60/APP30/BF10, and PP55/APP30/BF15 in **Figure 3**. It is possible that BF

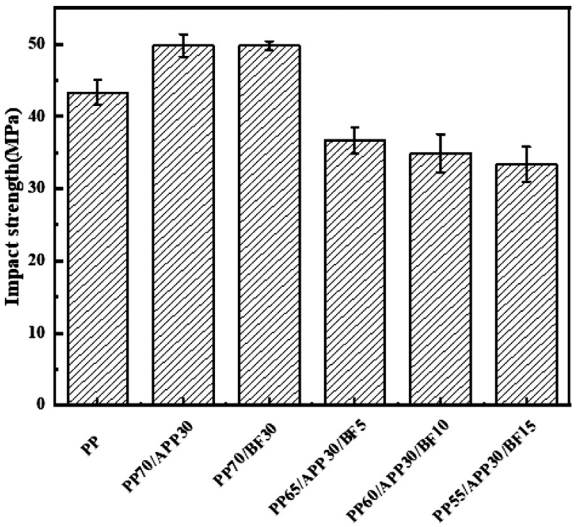

FIGURE 4 | Impact strength of PP and composites.

was arranged in the matrix along the stress direction, resulting in the increase of the bending strength. It can be seen from **Figure 2-4** that the tensile strength and impact strength of the samples PP65/APP30/BF5, PP60/APP30/BF10, and PP55/APP30/BF15 were slightly decreased. This may be because the flame retardants cannot be well dispersed in the matrix, and agglomeration occurs in some places, and stress concentrations formed around the agglomerated particles. At the same time, due to the large particle size of the agglomerated particles, their compatibility with the matrix is poor. Therefore, the tensile strength and impact strength of the composites are reduced.

Thermal Performance

The DSC chart of PP and composite materials is shown in **Figure 5**, and the main data of the samples after DSC tests are listed in **Table 2**. As can be seen from **Figure 5** and **Table 2**, the crystallization temperature and melting temperature of pure PP were 109.6 and 144.7°C, respectively. When APP and BF were added separately, the crystallization temperature and melting temperature of the samples increased. This is due to the heterogeneous nucleation of APP or BF in the PP phase. PP or BF forms a crystal nucleus, which reduces the mobility of the PP molecular chain, thus leading to a higher crystallization temperature and melting temperature of the composite material. When APP and BF are mixed, there may have a hydrogen bonding which weakens heterogeneous nucleation to a certain extent (Kumar and Tumu, 2019; Ding et al., 2020; Yang et al., 2020). As the amount of BF addition increases, the crystallization temperature increased gradually. The crystallization temperatures of the samples PP65/APP30/BF5, PP60/APP30/BF10 and PP55/APP30/BF15 were 108.4, 110.9, and 111.4°C, and there was no significant change in the melting temperature of these samples.

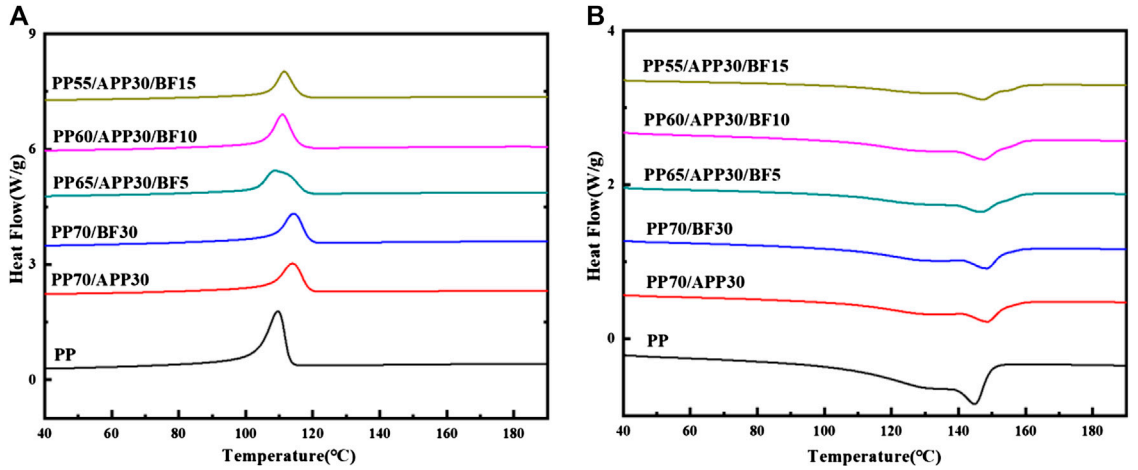

FIGURE 5 | DSC curves of PP and composites. (**(A)** cooling curves; **(B)** heating curves).

TABLE 2 | Main data of DSC tests obtained for PP and composites.

Samples	T_c (°C)	T_m (°C)
PP	109.6	144.7
PP70/APP30	114.1	148.7
PP70/BF30	114.5	148.4
PP65/APP30/BF5	108.4	147.2
PP60/APP30/BF10	110.9	147.7
PP55/APP30/BF15	111.4	147.7

T_c is the crystallization temperature of sample, T_m is the melting temperature of sample.

TABLE 3 | Results of flame-retardant test.

Samples	LOI/vol%	UL-94
PP	21 ± 0.5	No rating
PP70/APP30	33 ± 0.5	No rating
PP70/BF30	20 ± 0.5	No rating
PP65/APP30/BF5	33 ± 0.5	No rating
PP60/APP30/BF10	34 ± 0.5	V-2
PP55/APP30/BF15	32 ± 0.5	V-1

Flame Retardant Properties

The results of LOI and UL-94 vertical burning test are shown in **Table 3**. According to **Table 3**, pure PP had a LOI oxygen index of 21, which is easy to burn in air. The LOI of sample PP70/BF30 was 20, which was lower than the pure PP sample, indicating that the addition of BF promotes the flammability of PP. This result was confirmed by the TTI (time to ignition) value in the subsequent cone test, because the BF is a flammable material which reduces the thermal stability of BF/PP. The LOI values of samples PP65/APP30/BF5, PP60/APP30/BF10, and PP55/APP30/BF15 were 33, 34, and 32, respectively. This indicates that the presence of APP, the LOI value of these samples is not significantly affected as the content of BF increases. It can be seen from the UL-94 grade listed in **Table 3** that adding BF or APP alone does not achieve a higher flame-retardant grade of PP. When the content of APP in the sample is 30%, the UL-94 grade of the sample increased as the content of BF increases. The UL-94 grades of samples PP65/APP30/BF5, PP60/APP30/BF10, and PP55/APP30/BF15 were no rating, V-2, and V-1, respectively. The samples which added both APP and BF showed a dense carbon layer after combustion. This indicates that the addition of BF can effectively improve the flame retardancy of PP/APP composites and promote the formation of charcoal.

Thermal Stability Test

The TGA and DTG curves of samples are shown in **Figure 6**. Pure PP begins to decompose at around 320°C and the maximum decomposition temperature (T_{max}) was 450°C. Due to the poor thermal stability of BF, the PP70/BF30 composite had poor stability. **Figure 7A** shows that the sample PP70/BF30 underwent two stages of the pyrolysis and decomposition of residual carbon. The main peak between 340 and 370°C was assigned to the degradation of a-cellulose (Lewin and Basch, 1978). This sample has almost no residue at 700°C. This result shows that adding BF or APP reduced the initial decomposition temperature of the samples. Because APP is thermally decomposed to form ammonium polymetaphosphate, it promotes the decomposition of BF and the matrix to form a carbon layer covering the surface of the substrate. It can be seen from the DTG curve that when BF or APP was added, the temperature corresponding to the maximum decomposition rate of the sample moves in the direction of a high temperature. The temperature corresponding to the maximum decomposition rate of the PP65/APP30/BF5, PP60/APP30/BF10, and PP55/APP30/BF15 increased to 483, 485, and 491°C, respectively. This is probably due to the fact that when APP and BF were added into PP, the samples formed a highly stable carbon layer under the flame which can protect the matrix from further decomposition. The residue data of the thermogravimetric analysis was consistent with the residue data after the cone test. Pure PP residue content was only 0.5% at 700°C, while the residue content of the PP55/APP30/BF15 sample was as high as 11.4%, as shown in **Table 4**. This indicates that the addition of APP and BF allows PP to form a dense protective carbon layer.

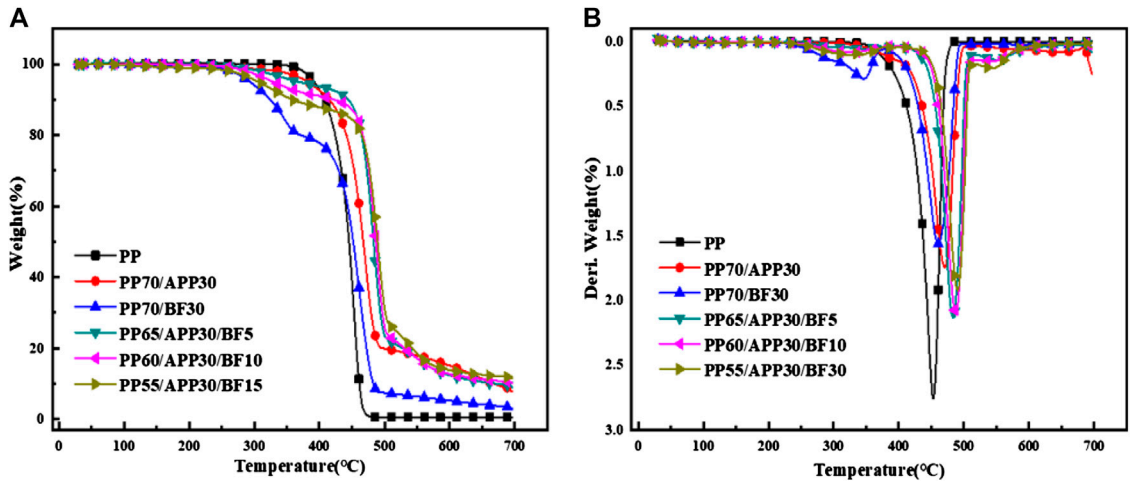

FIGURE 6 | TGA **(A)** and DTG **(B)** curves of PP and composites.

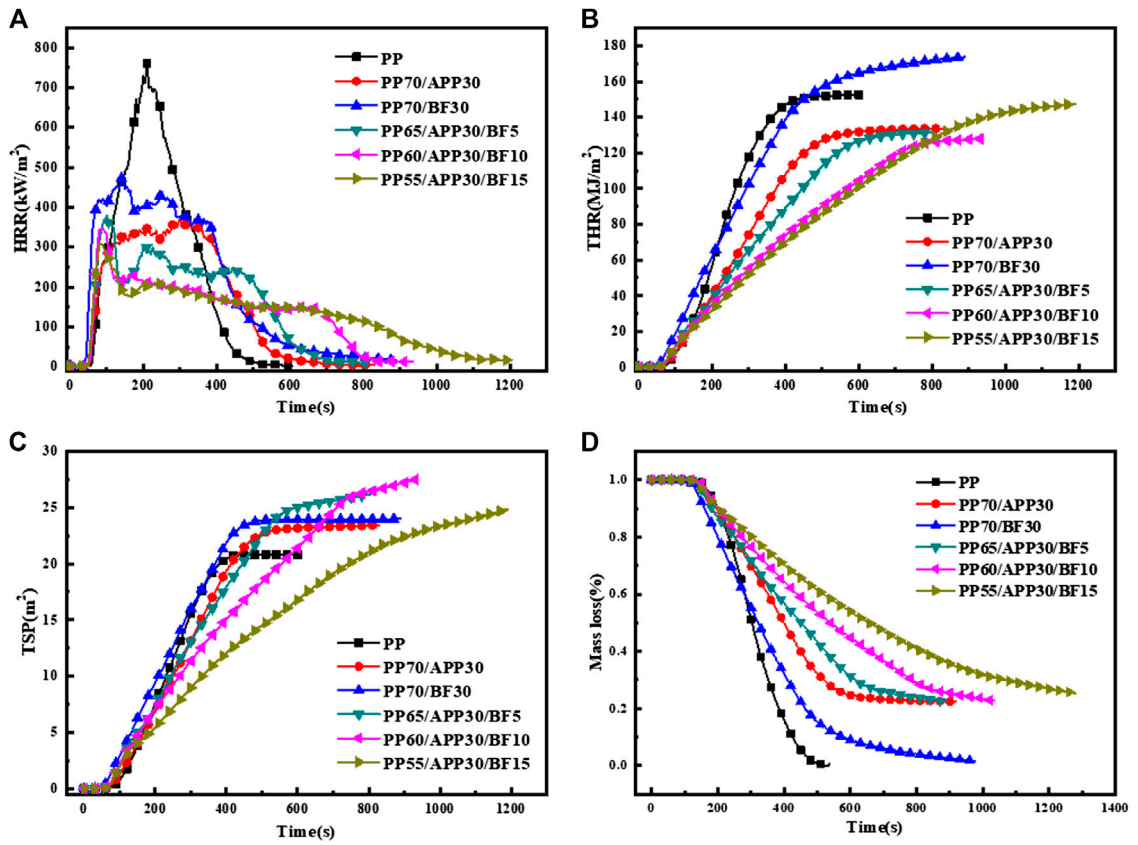

FIGURE 7 | HRR **(A)**, THR **(B)**, TSP **(C)**, and Mass loss **(D)** curves of PP and composites.

Cone Calorimeter Test

The graph of the cone calorimeter test is shown in **Figure 7** and the main data is listed in **Table 5**. The cone calorimeter test can truly reflect the level of material burning and can derive many combustion characteristics (Nie et al., 2008). From **Figure 6A**, it can be seen that the PP sample had a sharp and high peak at a heat flux of 35 kW/m^2, this shows that pure PP will burn quickly and release more heat in a short time. Within 400 s, the peak heat

TABLE 4 | TGA data obtained for PP and composites.

Samples	$T_{1wt\%}$ (°C)	$T_{5wt\%}$ (°C)	T_{max} (°C)	Char residue at 700°C (wt%)
PP	364.38	391.95	451.12	0.5
PP70/APP30	273.25	381.79	472.87	7.8
PP70/BF30	240.43	288.72	464.96	2.6
PP65/APP30/BF5	277.82	361.91	483.82	8.7
PP60/APP30/BF10	261.79	324.48	485.63	9.9
PP55/APP30/BF15	177.99	301.24	491.84	11.4

TABLE 5 | Main data of cone calorimeter test of PP and composites.

Samples	PHRR (kW/m^2)	THR (MJ/m^2)^1	TSP (m^2)^2	Mass loss (%)	TTI (s)
PP	761.6	151.9	20.8	100	60 ± 1
PP70/APP30	373.4	127.1	22.7	78	57 ± 1
PP70/BF30	472.4	156.8	23.9	99	46 ± 1
PP65/APP30/BF5	379.4	112.6	22.6	78	55 ± 1
PP60/APP30/BF10	346.3	90.0	18.4	77	56 ± 1
PP55/APP30/BF15	308.2	86.2	14.5	75	52 ± 1

THR (MJ/m^2)^1 means total heat release of sample at 500 s; TSP (m^2)^2 means total smoke production of sample at 500 s.

release rate (PHRR) reached 761.6 kW/m^2 and the total heat release (THR) was 146 MJ/m^2 (**Figure 6B**). The PHRR of samples PP70/APP30, PP70/BF30, and PP55/APP30/BF15 was reduced to 373.4, 472.4, and 308.2 kW/m^2, respectively. The PP55/APP30/BF15 (APP/BF = 2:1) sample had the lowest PHRR, and this indicates that the BF and APP have an obvious synergistic flame-retardant effect in PP. The result shows that the flame-retardant effect of PP55/APP30/BF15 is the best. This is due to the fact that APP and BF have a certain synergistic effect and a dense carbon layer formed during the combustion process. This carbon layer can effectively block the entry of oxygen and the release of heat, thus reducing the PHRR of the sample. It can be seen from **Figure 6A** that the burning time of PP55/APP30/BF15 was significantly longer than that of pure PP. It is due to the decomposition of transient carbon (Bai et al., 2014). To a certain extent, the addition of APP and BF can effectively inhibit the spread of the flame and reduce the risk factor of fire.

When the test sample is pyrolyzed under the condition of heat radiation, the local concentration of released flammable volatiles reaches the lower limit of flammability, and combustion occurs (Monti and Camino, 2013). **Table 5** shows that the addition of additives reduces the time to ignition (TTI) of the samples. The TTI of the pure PP was 60 s and in the PP70/BF30 sample it was 46 s. The TTI of samples with BF additive alone was 14 s ahead of the pure PP. The addition of BF had the greatest influence on the flame retardancy of all samples and this result was substantiated in the thermogravimetric data. When APP was added, the TTI of the PP55/APP30/BF15 sample was extended and ignited at 52 s. This is due to the presence of an expanded carbon layer in the presence of APP which covered the surface of the substrate and prolonged the ignition time. It can be seen from **Figure 6B** that the THR slope of samples PP65/APP30/BF5, PP60/APP30/BF10, and PP55/APP30/BF15 gradually slows down with the increase of flame-retardant content. Within 500 s, the THR of PP55/APP30/BF15 was only 86.2 MJ/m^2, while in PP it was 151.9 MJ/m^2. Compared with PP, the THR of PP55/APP30/BF15 decreased 43.3%. The slope of the THR curve can reflect the spread fire of samples. This result proves that the combination of APP and BF can effectively inhibit the generation of heat.

When a fire occurs, the mortality caused by smoke is more than that caused by flame. According to reports, about 50% of those trapped in a fire were killed by inhaling toxic gases instead of from fire damage (Manfredi et al., 2006; Manfredi et al., 2010). The initial 500 s is of great significance for escaping a fire (Araby et al., 2018; Kruger et al., 2019; Blais et al., 2020). The total smoke production (TSP) curve, as shown in **Figure 6C,** indicates that the TSP values of samples where flame retardant were added, are more than, or close to those of the pure PP within 500 s except for the PP55/APP30/BF15 sample. The TSP value of the PP55/APP30/BF15 sample was 14.5 m^2 which is 30.3% lower than PP. Decreasing the value of TSP can improve the smoke suppression effect. The reason "why the smoke suppression effect of the PP55/APP30/BF15 sample is so significant" (Dong et al., 2012; Sun et al., 2020; de Juan et al., 2020) is that the synergistic action of BF and APP in the combustion process is within 500 s. This process formed a dense and porous structure of sintered carbon. This was confirmed by the SEM image of the carbon residue after the cone test. This result shows that APP and BF added in PP significantly promotes the formation of residues. Cone test results show that the residue content of the PP55/APP30/BF15 sample reached 25%, but the pure PP had no residue formation. It can be seen from **Figure 6D** that the PP55/APP30/BF15 sample has the lowest mass loss and the highest residual amount. This indicates that the APP/BF system effectively forms an expanded and dense carbon layer. The carbon layer protects the underlying substrate from rapid degradation and reduces the release of combustible gases during combustion. Thereby, the residual carbon after burning was increased.

Microscopic Characterization

The digital photos of samples after the cone calorimeter test are shown in **Figure 8**. There was almost no residue after the combustion of pure PP as shown in **Figure 8A**. This is because PP is a polyolefin compound and will burn completely when it is ignited. APP can promote PP to form a continuous and expanded carbon layer as shown in **Figure 8B**. However, the addition of BF into PP only formed a small amount of gray charcoal, as shown in **Figure 8C**. When the content of APP is 30%, as the content of BF increases, the carbon layer becomes denser and denser. There are no macro-cracks in the carbon layer, as shown in **Figure 8E**. When combustion occurs, APP will decompose to produce acidic substances such as polyphosphoric acid, which quickly dehydrates the carbon source (BF) into char. The formed carbon layer is continuous and dense, which can be observed in **Figure 8**. The results in **Figure 8** show that the addition of BF and APP into PP can effectively promote char formation. BF and APP had a good synergistic flame-retardant effect and had a certain cross-linking effect.

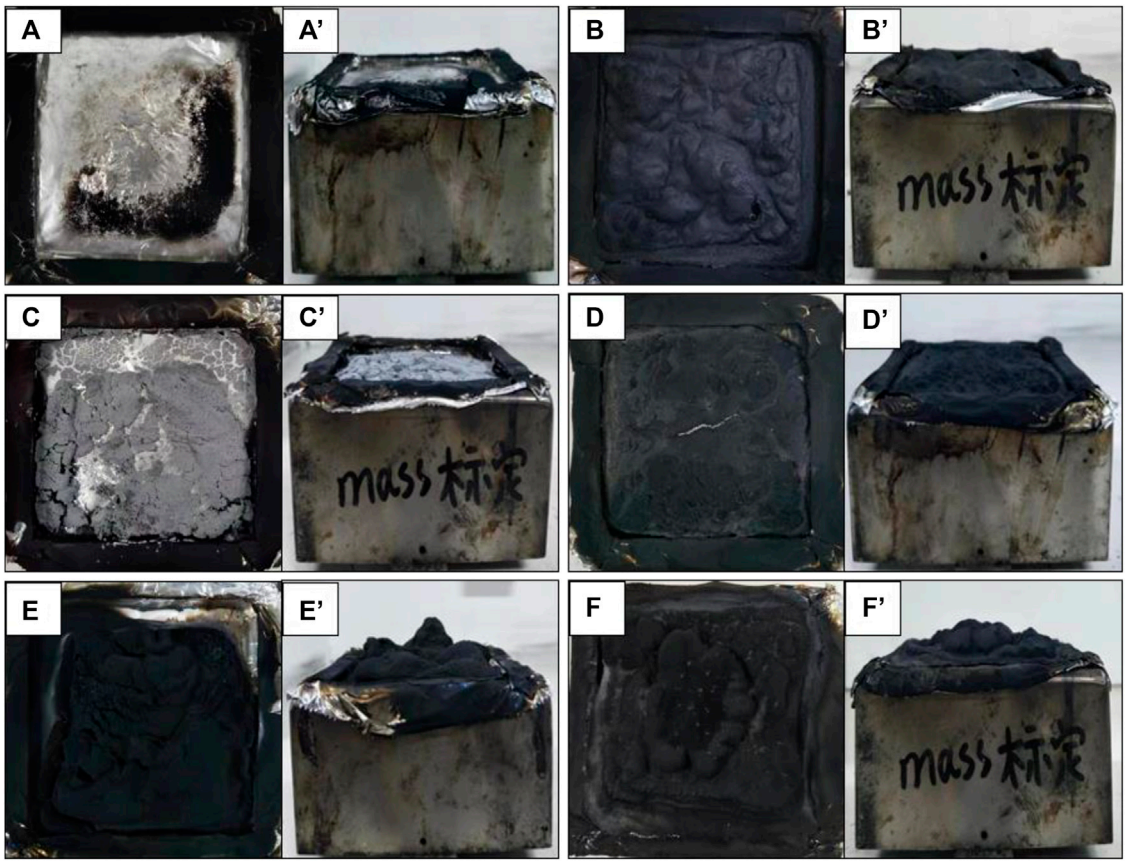

FIGURE 8 | Digital photo of surface intumescent carbon layer of PP and composites after cone calorimeter test. (**(A,A')** PP; **(B,B')** PP70/APP30; **(C,C')** PP70/BF30; **(D,D')** PP65/APP30/BF5; **(E,E')** PP60/APP30/BF10; **(F,F')** PP55/APP30/BF15).

In order to observe the microscopic morphology of the carbon layer, residue after the cone calorimeter test was observed by SEM. Since there was almost no residue formation after the cone test of pure PP, no observation was made for pure PP. It can be seen from **Figure 9** that although the microstructure of the carbon residue of the PP70/APP30 sample was relatively smooth and continuous, the carbon layer as a whole was brittle. It can be seen from **Figure 9B** that by adding 30% BF alone, the carbonation effect of the sample was poor, and the continuous carbon layer did not form.

After compounding BF 5, 10, 15, and 30% into APP, it can be seen from the SEM image that the continuity and compactness of the carbon layer are gradually increased in **Figures 9C–E**. The pores in the carbon layer became smaller and smaller. The morphology of the carbon residue shows a rough and convex appearance. These protrusions had many micropores which greatly increased the specific surface area of the carbon layer. At the same time, a cross-linking network was formed between the protrusions, so the stability of the carbon layer was improved. The carbon layer can effectively suppress the spread of heat. As shown in **Figure 9E**, the existence of many microporous structures in the carbon layer may be a significant cause of the smoke suppression effect, because these micro-holes may absorb part of the smoke.

CONCLUSIONS

A series of flame-retardant PP composites with a certain ratio of BF and APP were prepared. BF was used as a synergistic smoke suppressant. The influence of BF and APP as flame retardants on PP was studied. The addition of BF alone will improve the comprehensive mechanical properties of PP. However, when the APP and BF were mixed, the particles will agglomerate due to the higher amount of the addition. They will reduce some mechanical properties of PP. DSC results showed that the addition of BF in PP produced heterogeneous nucleation and affected the crystallization behavior of the composites. When the ratio of APP to BF was 2:1 and the total addition amount was 45%, the smoke suppression effect was most significant. The amount of carbon residue reached 25%. TGA and DTG data show that the PP55/APP30/BF15 sample had the highest amount of carbon residue with 11.4%, while pure PP had almost no carbon residue generation. The results of cone calorimetry show that the PHRR, THR, and mass loss of the PP55/APP30/BF15 sample were significantly lower than that of the pure

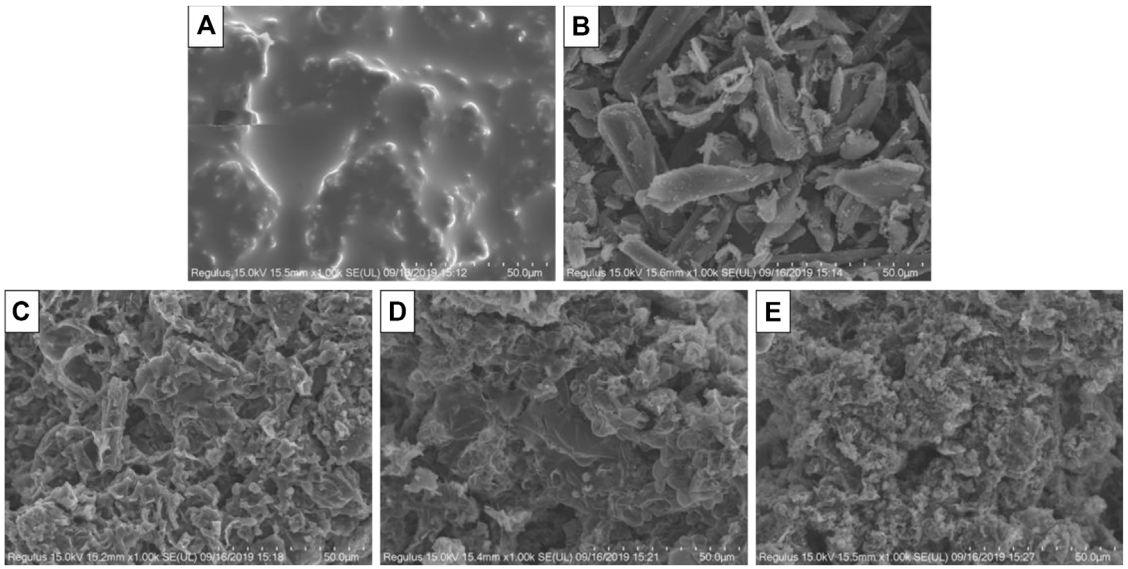

FIGURE 9 | SEM of surface carbon layer of composites after cone calorimeter test. (**(A)** PP70/APP30; **(B)** PP70/BF30; **(C)** PP65/APP30/BF5; **(D)** PP60/APP30/BF10; **(E)** PP55/APP30/BF15).

PP, from 761.6 to 308.2 kW/m^2, from 151.9 to 86.2 MJ/m^2, and from 100 to 75%, respectively. The SEM and the digital photos of residual carbon show that the PP55/APP30/BF15 sample formed a dense and continuous carbon layer, which hinders the transfer of heat and flammable gases into the matrix. The carbon layer had many convex structures, which contains many tiny holes that may absorb a large amount of smoke. Thus, the PP55/APP30/BF15 sample exhibited a better smoke suppression effect. Therefore, it substantiates that the combination of APP and BF is a potential application for PP with flame retardancy and smoke suppression.

DATA AVAILABILITY STATEMENT

All datasets presented in this study are included in the article/supplementary material.

AUTHOR CONTRIBUTIONS

YL and HL designed and performed the experiment, YL wrote the paper, HL, QC, FL, and CC edited the paper.

FUNDING

This work was supported by the foundation of Quangang Petrochemical Research Institute, Fujian Normal University (No. 2018YJY03); the Science and Technology Development Projects of the Central Committee Guidance Local (2018L3015); the Startup Fund from Fujian Normal University; the Fujian Provincial Department of Science and Technology (2018Y4002); and the National Natural Science Foundation of China (51903049).

REFERENCES

Abu Bakar, M. B., Mohd Ishak, Z. A., Mat Taib, R., Rozman, H. D., and Mohamad Jani, S. (2010). Flammability and mechanical properties of wood flour-filled polypropylene composites. *J. Appl. Polym. Sci.* 116 (5), 2714–2722. doi:10.1002/app.31791

Araby, S., Wang, C.-H., Wu, H., Meng, Q., Kuan, H.-C., Kim, N. K., et al. (2018). Development of flame-retarding elastomeric composites with high mechanical performance. *Compos. Appl. Sci. Manuf.* 109, 257–266. doi:10.1016/j.compositesa.2018.03.012

Bai, G., Guo, C., and Li, L. (2014). Synergistic effect of intumescent flame retardant and expandable graphite on mechanical and flame-retardant properties of wood flour-polypropylene composites. *Construct. Build. Mater.* 50, 148–153. doi:10.1016/j.conbuildmat.2013.09.028

Blais, M. S., Carpenter, K., and Fernandez, K. (2020). Comparative room burn study of furnished rooms from the United Kingdom, France and the United States. *Fire Technol.* 56 (2), 489–514. doi:10.1007/s10694-019-00888-8

Chattopadhyay, S. K., Khandal, R. K., Uppaluri, R., and Ghoshal, A. K. (2011). Bamboo fiber reinforced polypropylene composites and their mechanical, thermal, and morphological properties. *J. Appl. Polym. Sci.* 119 (3), 1619–1626. doi:10.1002/app.32826

De Juan, S., Zhang, J. H., Acuna, Pablo., Nie, S. B., and Liu, Z. Q. (2020). An efficient approach to improving fire retardancy and smoke suppression for intumescent flame-retardant polypropylene composites via incorporating organo-modified sepiolite. *Fire Mater.* 43 (8), 961–970. doi:10.1002/fam.2757

Ding, C. X., Pan, M. Z., Chen, H., Zhang, S., and Mei, C. (2020). An anionic polyelectrolyte hybrid for wood-polyethylene composites with high strength and fire safety via self-assembly. *Construct. Build. Mater.* 248, 1–12. doi:10.1016/j.conbuildmat.2020.118661

Dong, H., Yuan, B., Qi, C., Li, K., Shang, S., Sun, Y., et al. (2020). Preparation of piperazine cyanurate by hydrogen-bonding self-assembly reaction and its application in intumescent flame-retardant polypropylene composites. *Polym. Adv. Technol.* 31 (5), 1027–1037. doi:10.1002/pat.4837

Dong, Y. Y., Gui, Z., Hu, Y., Wu, Y., and Jiang, S. H. (2012). The influence of titanate nanotube on the improved thermal properties and the smoke

suppression in poly (methyl methacrylate). *J. Hazard Mater.* 209, 34–39. doi:10.1016/j.jhazmat.2011.12.048.

Fang, L., Lu, X. Z., Zeng, J., Chen, Y., and Tang, Q. (2020). Investigation of the flame-retardant and mechanical properties of bamboo fiber-reinforced polypropylene composites with melamine pyrophosphate and aluminum hypophosphite addition. *Materials* 13 (2), 479. doi:10.3390/ma13020479

Kong, Q. H., Sun, Y. L., Zhang, C. J., Guan, H., Zhang, J., Wang, D.-Y., et al. (2019). Ultrathin iron phenyl phosphonate nanosheets with appropriate thermal stability for improving fire safety in epoxy. *Compos. Sci. Technol.* 182, 107748. doi:10.1016/j.compscitech.2019.107748

Krüger, S., Schartel, B., Schubert, M., and Schoch, R. (2019). Wood plastic composites: how do flame retardant influence the smoke gas composition in case of fire?. *Bautechnik* 96 (6), 438–449. doi:10.1002/bate.201900020

Kumar, A., and Tumu, V. R. (2019). Physicochemical properties of the electron beam irradiated bamboo powder and its bio-composites with PLA. *Compos. B. Engg.* 175, 107098. doi:10.1016/j.compositesb.2019.107098

Kumar, N., Mireja, S., Khandelwal, V., Arun, B., and Manik, G. (2017). Light-weight high-strength hollow glass microspheres and bamboo fiber based hybrid polypropylene composite: a strength analysis and morphological study. *Compos. B. Eng.* 109, 277–285. doi:10.1016/j.compositesb.2016.10.052

Lee, S.-Y., Chun, S.-J., Doh, G.-H., Kang, I.-A., Lee, S., and Paik, K.-H. (2009). Influence of chemical modification and filler loading on fundamental properties of bamboo fibers reinforced polypropylene composites. *J. Compos. Mater.* 43 (15), 1639–1657. doi:10.1177/0021998309339352

Lewin, M., and Basch, A. (1978). *Structure, pyrolysis, and flammability of cellulose*. New York, NY: Plenum Press, Vol. 2: 1–41.

Li, W., He, X., Zuo, Y., Wang, S., and Wu, Y. (2019). Study on the compatible interface of bamboo fiber/polylactic acid composites by *in-situ* solid phase grafting. *Int. J. Biol. Macromol.* 141, 325–332. doi:10.1016/j.ijbiomac.2019.09.005

Manfredi, L. B., Rodríguez, E., Wladyka-Przybylak, M., and Vázquez, A. (2010). Thermal properties and fire resistance of jute-reinforced composites. *Compos. Interfaces.* 17 (5–7), 663–675. doi:10.1163/092764410x513512

Manfredi, L. B., Rodríguez, E. S., Wladyka-Przybylak, M., and Vázquez, A. (2006). Thermal degradation and fire resistance of unsaturated polyester, modified acrylic resins and their composites with natural fibres. *Polym. Degrad. Stab.* 91 (2), 255–261. doi:10.1016/j.polymdegradstab.2005.05.003

Monti, M., and Camino, G. (2013). Thermal and combustion behavior of polyethersulfone-boehmite nanocomposites. *Polym. Degrad. Stab.* 98 (9), 1838–1846. doi:10.1016/j.polymdegradstab.2013.05.010

Nie, S., Hu, Y., Song, L., He, Q., Yang, D., and Chen, H. (2008). Synergistic effect between a char forming agent (CFA) and microencapsulated ammonium polyphosphate on the thermal and flame retardant properties of polypropylene. *Polym. Adv. Technol.* 19 (8), 1077–1083. doi:10.1002/pat.1082

Nie, S., Liu, X., Wu, K., Dai, G., and Hu, Y. (2013). Intumescent flame retardation of polypropylene/bamboo fiber semi-biocomposites. *J. Therm. Anal. Calorim.* 111 (1), 425–430. doi:10.1007/s10973-012-2422-3

Shi, Y. Q., Liu, C., Liu, L., Fu, L., Yu, B., Lv, Y., et al. (2019). Strengthening, toughing and thermally stable ultra-thin MXene nanosheets/polypropylene nanocomposites via nanoconfinement. *Chem. Eng. J.* 378, 122267. doi:10.1016/j.cej.2019.122267

Sun, L. C., Xie, Y. J., Ou, R, X., Guo, C. G., Hao, X. L., et al. (2020). The influence of double-layered distribution of fire retardants on the fire retardancy and mechanical properties of wood fiber polypropylene composites. *Constr. Build Mater.* 242, 1–8. doi:10.1016/j.conbuildmat.2020.118047.

Tang, G., Liu, X., Yang, Y., Chen, D., Zhang, H., Zhou, L., et al. (2020a). Phosphorus-containing silane modified steel slag waste to reduce fire hazards of rigid polyurethane foams. *Adv. Powder Technol.* 31 (4), 1420–1430. doi:10.1016/j.apt.2020.01.019

Tang, G., Liu, X., Zhou, L., Zhang, P., Deng, D., and Jiang, H. (2020b). Steel slag waste combined with melamine pyrophosphate as a flame retardant for rigid polyurethane foams. *Adv. Powder Technol.* 31 (1), 279–286. doi:10.1016/j.apt.2019.10.020

Tang, G., Zhou, L., Zhang, P., Han, Z., Chen, D., Liu, X., et al. (2020c). Effect of aluminum diethylphosphinate on flame retardant and thermal properties of rigid polyurethane foam composites. *J. Therm. Anal. Calorim.* 140 (2), 625–636. doi:10.1007/s10973-019-08897-z

Wang, J. S., Xue, L., Zhao, B., Lin, G., Jin, X., Liu, D., et al. (2020). Flame retardancy, fire behavior, and flame retardant mechanism of intumescent flame retardant EPDM containing ammonium polyphosphate/pentaerythrotol and expandable graphite. *Materials* 12 (24), 4035. doi:10.3390/ma12244035

Wang, L., Yang, W., Wang, B., Wu, Y., Hu, Y., Song, L., et al. (2012). The impact of metal oxides on the combustion behavior of ethylene-vinyl acetate coploymers containing an intumenscent flame retardant. *Ind. Eng. Chem. Res.* 51 (23), 7884–7890. doi:10.1021/ie202502s

Wu, K., Wang, X. Y., Xu, Y. H., and Guo, W. (2020a). Flame retardant efficiency of modified para-aramid fiber synergizing with ammonium polyphosphate on PP/EPDM. *Polym. Degrad. Stab.* 172, 1090605. doi:10.1016/j.polymdegradstab.2019.109065

Wu, Q., Guo, J., Fei, B., Li, X., Sun, J., Gu, X., et al. (2020b). Synthesis of a novel polyhydroxy triazine-based charring agent and its effects on improving the flame retardancy of polypropylene with ammonium polyphosphate and zinc borate. *Polym. Degrad. Stab.* 175, 109–123. doi:10.1016/j.polymdegradstab.2020.109123

Xu, S., Zhang, M., Li, S., Yi, M., Shen, S., Zeng, H., et al. (2019). Non-isothermal decomposition kinetic of polypropylene/hydrotalcite composite. *J. Nanosci. Nanotechnol.* 19 (11), 7493–7501. doi:10.1166/jnn.2019.16675

Xu, X. D., Dai, J. F., Ma, Z. W., Liu, L., Zhang, X., Liu, H., et al. (2020). Manipulating interphase reactions for mechanically robust, flame-retardant and sustainable polylactide biocomposites. *Compos. B. Eng.* 190, 107903. doi:10.1016/j.compositesb.2020.107930

Yang, J. W., Ji, G. Z., Gao, Y., Fu, W., Irfan, M., Mu, L., et al. (2020). High-yield and high-performance porous biochar produced from pyrolysis of peanut shell with low-dose ammonium polyphosphate for chloramphenicol adsorption. *J. Clean. Prod.* 264, 121516. doi:10.1016/j.jclepro.2020.121516

Yang, W., Lu, H., Tai, Q., Qiao, Z., Hu, Y., Song, L., et al. (2011). Flame retardancy mechanisms of poly(1,4-butylene terephthalate) containing microencapsulated ammonium polyphosphate and melamine cyanurate. *Polym. Adv. Technol.* 22 (12), 2136–2144. doi:10.1002/pat.1735

Yu, B., Yuen, A. C. Y., Xu, X., Zhang, Z. C., Yang, W., Lu, H., et al. (2020). Engineering MXene surface with POSS for reducing fire hazards of polystyrene with enhanced thermal stability. *J. Hazard Mater.* 401, 123342. doi:10.1016/j.jhazmat.2020.123342

Zhao, Z., Jin, Q., Zhang, N., Guo, X., and Yan, H. (2018). Preparation of a novel polysiloxane and its synergistic effect with ammonium polyphosphate on the flame retardancy of polypropylene. *Polym. Degrad. Stab.* 150, 73–85. doi:10.1016/j.polymdegradstab.2018.02.007

Zhou, L., Guo, C., and Li, L. (2011). Influence of ammonium polyphosphate modified with 3-(Methylacryloxyl) propyltrimethoxy silane on mechanical and thermal properties of wood flour-polypropylene composites. *J. Appl. Polym. Sci.* 122 (2), 849–855. doi:10.1002/app.34069

Conflict of Interest: The authors declare that the research was conducted in the absence of any commercial or financial relationships that could be construed as a potential conflict of interest.